Accepted Manuscript

Title: Synthesis of dihydropyrazole sulphonamide derivatives that act as anti-cancer agents through COX-2 inhibition

Author: Han-Yue Qiu Peng-Fei Wang Zhen Li Jun-Ting Ma Xiao-Ming Wang Yong-Hua Yang Hai-Liang Zhu

PII: S1043-6618(15)00292-3
DOI: http://dx.doi.org/doi:10.1016/j.phrs.2015.12.025
Reference: YPHRS 3018

To appear in: *Pharmacological Research*

Received date: 9-8-2015
Revised date: 20-12-2015
Accepted date: 20-12-2015

Please cite this article as: Qiu Han-Yue, Wang Peng-Fei, Li Zhen, Ma Jun-Ting, Wang Xiao-Ming, Yang Yong-Hua, Zhu Hai-Liang.Synthesis of dihydropyrazole sulphonamide derivatives that act as anti-cancer agents through COX-2 inhibition.*Pharmacological Research* http://dx.doi.org/10.1016/j.phrs.2015.12.025

Synthesis of dihydropyrazole sulphonamide derivatives that act as anti-cancer agents through COX-2 inhibition

Han-Yue Qiu[†], Peng-Fei Wang[†], Zhen Li, Jun-Ting Ma, Xiao-Ming Wang*, Yong-Hua Yang*, Hai-Liang Zhu*

State Key Laboratory of Pharmaceutical Biotechnology, Nanjing University, Nanjing 210046, People's Republic of China

*Corresponding author. Tel. & fax: +86-25-83592672; e-mail: zhuhl@nju.edu.cn, yangyh@nju.edu.cn

†These two authors contributed equally to this paper.

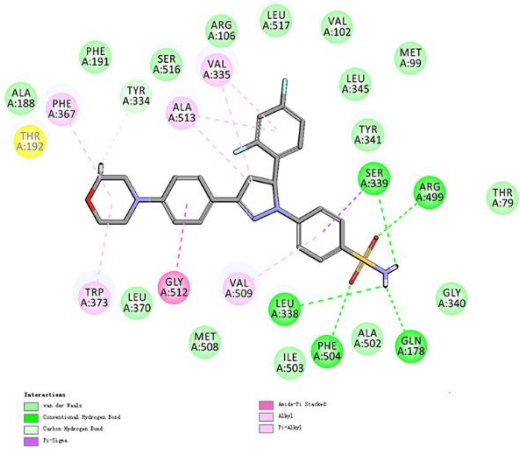

A series of novel COX-2 inhibitors was designed and synthesized as antitumor agents based on the knowledge of known COX-2 inhibitors and *in silico* scaffold modification strategy.

Abstract

COX-2 has long been exploited in the treatment of inflammation and relief of pain; however, research increasingly suggests COX-2 inhibitors might possess potential benefits to thwart tumour processes. In the present study, we designed a series of novel COX-2 inhibitors based on analysis of known inhibitors combined with an *in silico* scaffold modification strategy. A docking simulation combined with a primary screen

in vitro were performed to filter for the lead compound, which was then substituted, synthesized and evaluated by a variety of bioassays. Derivative **4d** was identified as a potent COX-2 enzyme inhibitor and exerted an anticancer effect through COX-2 inhibition. Further investigation confirmed that **4d** could induce A549 cell apoptosis and arrest the cell cycle at the G2/M phase. Moreover, treatment with **4d** reduced A549 cell adhesive ability and COX-2 expression. The morphological variation of treated cells was also visualized by confocal microscopy. Overall, the biological profile of **4d** suggests that this compound may be developed as a potential anticancer agent.

Keywords:

Dihydropyrazole

COX-2 selectivity

Antitumor

Diarylheterocycle

1 Introduction

Cyclooxygenase (COX), which is known for its rate-limiting role in the conversion of arachidonic acid to prostaglandin (PG), is generally classified into three subtypes: COX-1, COX-2 and COX-3.(1) The isoforms differ not only in expression but also in physiological and pathological functions. COX-1 is stimulated continuously in most normal tissues and COX-3 primarily in the central nervous system, while COX-2 is inducible. The amount of COX-2 often reaches a relatively high level when induced by stimuli such as pro-inflammatory cytokines, growth factors and tumour promoters, but it remains undetectable in most normal cells or tissues.(2-4) The significantly up-regulated expression of COX-2 in pathological processes revealed its involvement in diseases such as inflammation and various types of cancer. These characteristic variances in expression and distribution between COX-2 and other isoenzymes laid the foundation for designing COX-2-selective drugs that minimally disturb normal COX function.(5, 6) In practice, COX-2 has long been exploited to treat inflammation and relieve pain,(7-10) and along with continued research, interest in developing COX-2-specific antitumor medicaments is increasing considerably.(11-14) According to the database of clinical trials (www.clinicaltrials.gov), hundreds of clinical trials have been or are being conducted to test the anti-cancer potential of COX-2 inhibitors, mostly celecoxib (celebrex). The same repurposing strategy also applies to other known COX-2 inhibitors, providing a reference basis for COX-2-inhibitor-based anti-cancer drug development.(13, 15, 16) Given that there is a major discrepancy between supply and demand of anti-cancer agents, it is important to expand the availability of various types

of anti-cancer medicines. Therefore, in this study we attempted to design a class of COX-2-selective agents and assess their potential in anti-cancer agent development.

In general, selective COX-2 inhibitors can be categorized as diarylheterocycles or non-diarylheterocycles, and the largest proportion of selective COX-2 inhibitors comprises diarylheterocycles with a five-membered core.(17-20) As illustrated in **Fig. 1**, the most famous Coxibs (COX-2 selective inhibitors) are unexceptionally composed of various five-membered heterocyclic cores and 1, 2-diarylsubstitution. Based on this knowledge, we exploited a new diarylheterocycle scaffold with a dihydropyrazole group as the five-membered core ring. Additionally, a sulphonamide group was attached to the *p*-position of one aryl ring, as many studies have indicated that this pharmacophore plays a crucial role in COX-2 selectivity.(21, 22) The scaffold was substituted to obtain a library of small molecules. Using virtual screening, the molecules were ranked according to the docking score. The best hits were selected and preliminarily screened *in vitro*. We then validated the lead compound, which possessed good COX-2 inhibitory activity and comparable binding energy with celecoxib in docking with the COX-2 enzyme (**Table 1**). Derivatives of the lead compound (**4a-4t**) were synthesized and evaluated by additional bioassays.

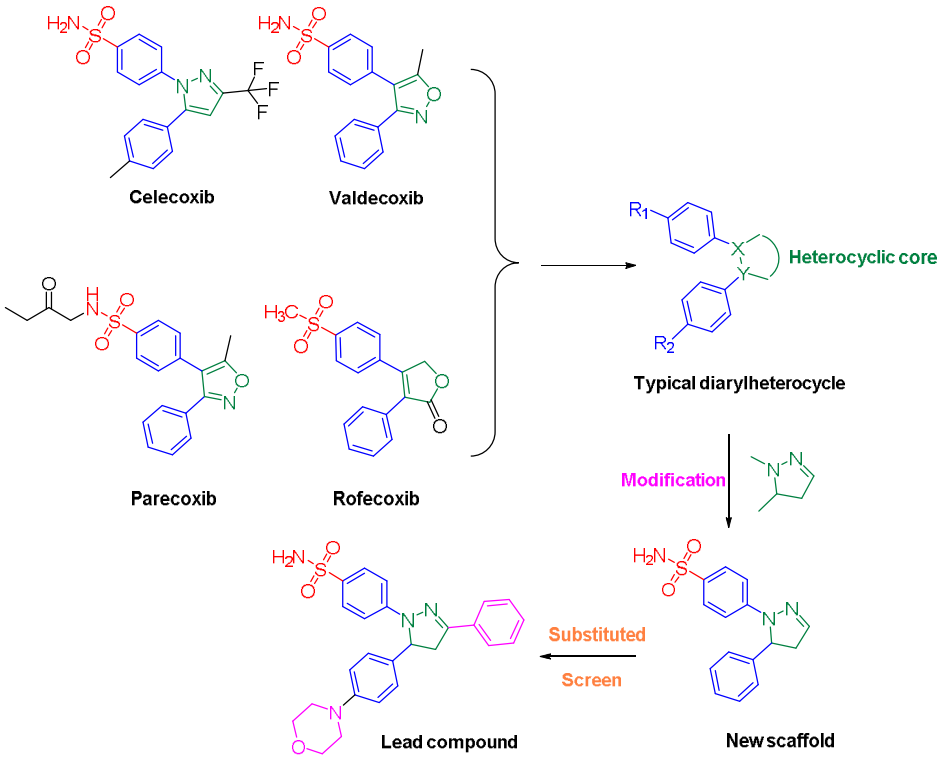

Fig. 1 Some well-known COX-2 inhibitors (coxibs) and the design pathway for novel dihydropyrazole sulphonamide derivatives.

Table 1. Interaction energy and AlogP of compounds **4a – 4t**

Compd	R	Interaction energy ΔG_b (kcal / mol))	AlogP[a]
Lead	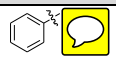	-58.44	3.736
4a	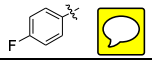	- 62.97	3.942
4b	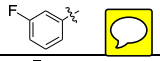	- 60.15	3.942
4c	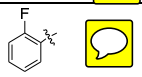	- 59.01	3.942
4d	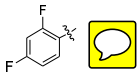	- 63.11	4.147
4e	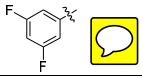	- 62.60	4.147
4f	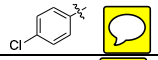	- 60.26	4.401
4g	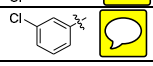	- 57.77	4.401
4h	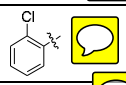	- 57.38	4.401
4i	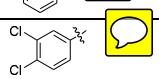	- 62.73	5.065
4j	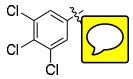	- 62.68	5.729

4k	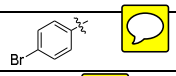	- 61.72	4.485
4l	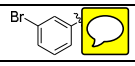	- 60.38	4.485
4m	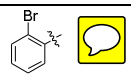	- 52.23	4.485
4n	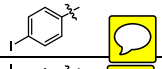	- 61.09	4.314
4o	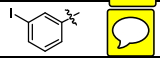	- 52.51	4.314
4p	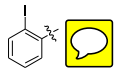	- 57.92	4.314
4q	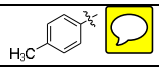	- 61.42	4.222
4r	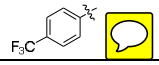	- 49.20	4.678
4s	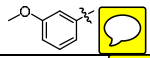	- 48.91	3.720
4t	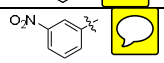	- 58.87	3.631
Celecoxib		- 56.13	5.946

[a] Calculated using Discovery Studio 3.5.

2 Materials and methods

2.1 Materials

All chemicals (reagent grade) used were purchased from Nanjing Chemical Reagent Co. Ltd. (Nanjing, China). Celecoxib was purchased from Sigma-Aldrich (St. Louis, MO). All the ^{1}H NMR spectra were recorded on a Bruker DPX 400 model spectrometer in DMSO-d_6, and chemical shifts (δ) are reported as parts per million (ppm). ESI-MS spectra were recorded by a Mariner System 5304 Mass spectrometer. Melting points were determined on a XT4 MP apparatus (Taike Corp, Beijing, China). Thin layer chromatography (TLC) was performed on silica gel plates (Silica Gel 60 GF254) and visualized in UV light (254 nm and 365 nm). Column chromatography was performed using silica gel (200-300 mesh) and eluting with ethyl acetate and petroleum ether (bp 30-60 °C).

The COX-1 (human) Inhibitor Screening Assay Kit (#701070) and COX-2 (human)

Inhibitor Screening Assay Kit (#701080) were purchased from Cayman Chemical, (MI, USA). The PTGS2 small interfering RNA kit was purchased from Ribobio (GuangZhou, China). RNase A (#EN0531) was purchased from Thermo Scientific, Fermentas (USA). The AnnexcinV-FITC cell apoptosis assay kit (#BA11100) was purchased from BIO-BOX (Nanjing, China). Fibronectin (#F1056) and laminin (#L2020) were purchased from Sigma-Aldrich (St. Louis, MO). COX-2 anti-body (#12282P) was purchased from Cell Signalling Technology (Beverly, MA, USA).

2.2 General procedure for the synthesis of compounds 4a-4t

A mixture of compound **3a-3t** (5 mmol), 4-hydrazinylbenzenesulfonamide (5 mmol) and glacial acetic acid (2 mL) in ethanol (20 mL) was refluxed for 8 h. Afterwards, the cooled reaction contents were poured into ice water, and the products were filtered and washed carefully with ice water and cool ethanol. The crude products were recrystallized from methanol to obtain pure compounds **4a-4t**.

2.3 Cell Culture

A human hepatoma cell line (HepG2), human lung adenocarcinoma epithelial cell line (A549), carcinoma of cervix cell line (HeLa) and human kidney epithelial cell (293T) were purchased from Nanjing Keygen Technology (Nanjing, China). Cells were maintained in Dulbecco's modified Eagle's medium (DMEM, Hyclone) (High Glucose) with L-glutamine supplemented with 10% foetal bovine serum (FBS, BI), 100 U/mL penicillin and 100 mg/mL streptomycin (Hyclone), and incubated at 37 °C in a

humidified atmosphere containing 5% CO_2.

2.4 COX inhibitor screening assay

The ability of compounds **4a-4t** to inhibit COX-1 and COX-2 was determined using COX inhibitor screening assay kits according to the instruction manual.(23) In brief, COX-1 or COX-2 enzyme was pre-incubated with test compounds at 0 μM, 1 μM, 10 μM and 100 μM in reaction buffer (0.1 M Tris-HCl, pH 8.0, 5 mM EDTA, 2 mM phenol and 1 μM heme) at 37 °C for 10 min. The reactions were initiated by adding arachidonic acid to a final concentration of 100 μM and incubated at 37 °C for 2 min. Afterwards, 1 M HCl was added to the reaction mixtures to stop the reaction, followed by one tenth the volume of saturated stannous chloride (50 mg/mL). The reaction mixtures were incubated for 5 min at room temperature, and the amount of prostaglandin E2 formed during the reaction was measured by enzyme immunoassay.(24)

2.5 Anti-proliferation assay

The anti-proliferative activities of the prepared compounds against the A549, Hela, HepG2, and 293T cell lines were evaluated using a standard (MTT)-based colorimetric assay with some modification.(25) Cell lines were grown to log phase in DMEM supplemented with 10% foetal bovine serum. Cell suspensions were prepared and 100 μL/well dispensed into 96-well plates to give 10^4 cells/well. The subsequent incubation was performed at 37 °C, 5% CO_2 atmosphere for 24 h to allow the cells to reattach. Subsequently, cells were treated with the target compounds at 0 μM, 1 μM, 10 μM and

100 μM in the presence of 10% FBS for 24 h. Afterwards, cell viability was assessed by the conventional 3-(4, 5-dimethylthiazol-2-yl)-2, 5-diphenyltetrazolium bromide (MTT) reduction assay carried out strictly according to the manufacturer's instructions (Sigma). The absorbance (OD_{570}) was read on an ELISA reader (Tecan, Austria). In all experiments, three replicate wells were used for each drug concentration. Each assay was performed at least three times.

2.6 Cell adhesion assay

For the cell adhesion assay, 96-well flat-bottom plates were coated with 50 μL fibronectin and laminin (10 μg/mL) at 4 °C for 12 h and then blocked with 0.2% BSA for 2 h at room temperature followed by washing three times. Afterwards, A549 cells treated with **4d** and celecoxib for 24 h each were plated to the coated wells (10^4 per well) and incubated at 37 °C, 5% CO_2 for 40 min. A549 cells were allowed to adhere to the coated surface, washed intensively with PBS three times to remove non-adherent cells, and then incubated in 5 μg/mL MTT in complete medium at 37 °C for 4 h. Next, MTT-treated cells were lysed in DMSO, and absorbance was measured on an ELISA reader (Tecan, Austria). Each assay was performed at least three times.

2.7 Cell apoptosis assay

Approximately 10^5 cells/well were plated in a 24-well plate and allowed to adhere. Subsequently, the medium was replaced with fresh culture medium containing compound **4d** at final concentrations of 0, 1, 3 and 10 μM. Non-treated wells received

an equivalent volume of ethanol (<0.1%). After 24 h, cells were trypsinized, washed in PBS and centrifuged at 2000 rpm for 5 min. The pellet was resuspended in 500 μL staining solution (containing 5 μL AnnexinV-FITC and 5 μL PI in Binding Buffer), mixed gently and incubated for 15 min at room temperature in dark. The samples were then analysed by a FACSCalibur flow cytometer (Becton Dickinson, San Jose, CA, USA).

2.8 Cell cycle analysis

Cells were plated in 6-well plates (10^6 cells per well) and incubated at 37 °C for 24 h. Exponentially growing cells were then incubated with compound **4d** at different concentrations (0, 1, 3 and 10 μM). After 24 hours, cells were centrifuged at 1500 rpm at 4 °C for 5 minutes, fixed in 70% ethanol at 4 °C for at least 12 hours and subsequently resuspended in phosphate buffered saline (PBS) containing 0.1 mg/mL RNase A and 5 mg/mL propidium iodide (PI). The cellular DNA content was measured by flow cytometry for cell cycle distribution analysis, plotting at least 10000 events per sample. The percentage of cells in the G0/G1, S and G2/M phases of the cell cycle were determined using Flowjo 7.6.1 software.

2.9 Confocal microscopy assay

A549 cells were incubated with 5 μM compound **4d** for 30 min at 37 °C and washed three times with Hepes buffer, then scanned under microscopy. Subsequently, cells were seeded on a cover glass-bottom confocal dish and allowed to adhere for at least 24 h.

After treatment with compound **4d** at 1, 3, or 10 μM for 8 h, A549 cells were washed with cold PBS three times and fixed in 4% paraformaldehyde for 20 min. Fixed cells were stained with 1 μg/mL DAPI for 15 min. Before scanning by microscopy, the staining solution was removed, the dishes were washed with methanol three times, and glycerin was added to the dishes for imaging. The nuclear morphology of A549 cells was observed under an Olympus confocal microscope.

2.10 Western blot analysis

The A549 cells on 6-well plates were rinsed twice with cold PBS and lysed in RIPA lysis buffer containing a protease inhibitor mixture at 1:100 dilution on ice for 30 min. The insoluble components of cell lysates were removed by centrifugation (4 °C, 12000 × *g*, 10 min), and protein concentrations were measured using a Pierce BCA protein assay kit. Proteins were separated by sodium dodecyl sulphate-polyacrylamide gel electrophoresis (SDS-PAGE) and transferred onto polyvinylidene difluoride (PVDF) membranes. Membranes were blocked using skim milk and then incubated with diluted anti-COX-2 primary antibody (1:1000 dilution) at 4 °C with gentle shaking overnight. After washing five times, membranes were incubated with secondary antibody (1:1000-1:3000 dilution) for 1 h at room temperature.

2.11 siRNA transfection

Transfections of siRNA (nonsense siRNA and PTGS2 siRNA) into A549 cells were carried out using Opti-MEM and Lipo2000 (Invitrogen, Carlsbad, CA) according to the

manufacturer's instructions. Lipo2000 and siRNA were diluted separately in Opti-MEM, mixed and incubated for 5 min. The mixture was then added to A549 cells cultured in 6-well plates or 96-well plates. The treated cells were cultured at 37 °C, 5% CO_2 atmosphere for 24 h. Subsequently, A549 cells in 6-well plates were harvested for Western blotting, and the transfected cells in 96-well plates were treated with drugs for another 24 h. Cell viability was determined by the MTT assay in 96-well plates as previously described.

2.12 Scaffold modification

Scaffold modification was achieved with the module Grow Scaffold in Discovery Studio (version 3.5). Following the protocol, the scaffold was docked into COX-2 (PDB code: 3LN1) binding site beforehand. The 3-position of the dihydropyrazole core and the unsubstituted aryl ring were then marked as sites to be substituted. After calculation, modified molecules were produced to generate a library of small molecules.

2.13 Docking simulation

Molecular docking of the compounds binding the three-dimensional X-ray structure of COX-2 (PDB code: 3LN1) was carried out using Discovery Studio (version 3.5) as implemented through the graphical user interface DS-CDOCKER protocol. The aforementioned compounds were constructed, minimized and prepared. The crystal structures of the protein complex were retrieved from the RCSB Protein Data Bank (http://www.rcsb.org/pdb/home/home.do). All bound waters and ligands were

eliminated from the protein. Molecular docking was performed by inserting molecules into the binding pocket of COX-2 based on the binding mode. The types of interactions between the docked protein with ligand-based pharmacophore model were analysed after the end of molecular docking.

3. Results

3.1 Chemistry

The synthesis of compounds **4a-4t** followed the general pathway outlined in **Scheme 1**. The target compounds were obtained in three steps as described in the experimental section. All of the synthetic compounds **4a-4t** are being reported for the first time (**Table 1**) and gave satisfactory analytical and spectroscopic data. ^{1}HNMR and ESI-MS spectra were in full accordance with the assigned structures, which are presented in the **Supplementary Material**.

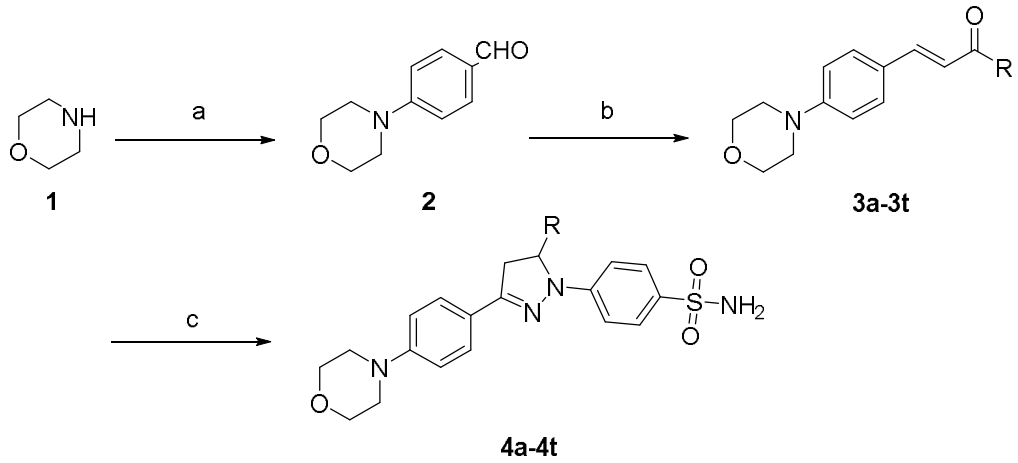

Scheme 1 (a) 1.0 equiv, 4-fluorobenzaldehyde, DMSO, 120 °C, 4 h; (b) 1.0 equiv, acetophenones, CH_3CH_2OH, 0 °C, 2 h; (c) 1.2 equiv, 4-hydrazinylbenzenesulfonamide, CH_3CH_2OH, 80 °C, 8 h.

3.2 Compound 4d selectively inhibited COX-2 activity

The ability of the tested compounds to inhibit human COX-1 and COX-2 was determined using COX inhibitor screening assay kits. The efficacies of the tested compounds were determined as the concentration causing 50% enzyme inhibition (IC_{50}) (**Table 2**). The majority of the tested compounds showed no inhibition of COX-1 up to 60 μM. However, a reasonable *in vitro* COX-2 inhibitory activity was observed with compounds **4d** with IC_{50} 0.08 ± 0.03 μM. The selectivity indices (COX-1/COX-2) were calculated and compared with that of the standard COX-2 selective inhibitor, celecoxib.

Table 2. Data from the in vitro COX-1/COX-2 enzyme inhibition assay of the designed compounds

Compd	IC_{50}±SD (μM)		Selectivity[b] Index (SI)
	COX-1	COX-2	
Lead	44.12± 0.26	0.11 ± 0.11	~ 401
4a	31.62 ± 0.13	1.23 ± 0.16	~ 26
4b	46.73 ± 0.01	2.67 ± 0.33	~ 18
4c	> 60	6.32 ± 0.68	> 9
4d	36.11 ± 0.56	0.08 ± 0.03	~ 451
4e	40.09 ± 0.19	0.11 ± 0.07	~ 364
4f	> 60	3.21 ± 0.18	> 19
4g	> 60	3.92 ± 0.36	> 15
4h	> 60	4.83 ± 0.44	> 12
4i	33.32 ± 1.06	0.17 ± 0.09	~ 196
4j	29.15 ± 0.29	0.31 ± 0.05	~ 94
4k	44.13 ± 0.73	0.92 ± 0.51	~ 48
4l	47.10 ± 0.51	1.68 ± 1.01	~ 28
4m	> 60	0.22 ± 0.24	> 273
4n	> 60	2.23 ± 0.59	> 27
4o	> 60	3.12 ± 0.51	> 19
4p	> 60	5.23 ± 1.13	> 11
4q	> 60	1.12 ± 0.17	> 54
4r	36.23 ± 0.06	0.24 ± 0.09	~ 151
4s	30.16 ± 0.34	0.19 ± 0.11	~ 159
4t	29.12 ± 0.53	0.14 ± 0.50	~ 208
Celecoxib	29.1 ± 0.12	0.07 ± 0.01	~ 415

[b] In vitro COX-2 selectivity index (IC_{50} COX-1 / IC_{50} COX-2).

3.3 Compound 4d inhibited cancer cell proliferation in a dose-dependent manner

All the compounds **4a-4t** were evaluated for their anti-proliferation activities against three cancer cell lines, HeLa (human cervix cell line), HepG2 (human liver cell line), A549 (human lungs cell line), and one non-cancer cell line, 293T (human kidney epithelial cell) by the MTT assay, and the calculated IC_{50} values are listed in **Table 3**. All compounds showed moderate to excellent anti-proliferative effects on A549 and Hela cancer cell lines but not on HepG2. Against the A549 cell line, compound **4d** showed the best anti-proliferative activity with lower IC_{50} value (1.63 ± 0.97 μM) compared with celecoxib (2.21 ± 1.31 μM). Subsequently, the MTT assay against one non-cancer cell line, 293T, was performed to test the cytotoxicity of the obtained compounds. As shown in **Table 3**, all the compounds have low cytotoxic effects on 293T, indicating a considerable safety profile.

Compound **4d** and celecoxib were further tested in COX-2 knockdown A549 cells with nonsense siRNA treated A549 cells used as control. Compared to the control group, the knockdown of COX-2 in A549 cells led to remarkable reduction of cell viability after drug treatment. The results are summarized in **Fig. 2** and demonstrate that the inhibitory action of compound **4d** against cancer cell proliferation is related to the level of COX-2.

Table 3. Proliferation inhibitory activities of compounds **4a-4t** against three cancer cell lines and cytotoxicity towards non-cancer cells

Compd	**IC_{50}±SD (μM)**			**CC_{50}±SD (μM)**
	A549	HeLa	HepG2	293T
Lead	3.18 ± 0.24	9.12± 0.32	18.15 ± 0.25	>100
4a	4.43 ± 0.31	10.37 ± 0.49	14.88 ± 0.87	>100
4b	6.29 ± 0.43	11.44 ± 0.34	20.51 ± 0.66	>100
4c	9.87 ± 1.01	22.7 ± 1.15	27.38 ± 1.34	>100
4d	1.63 ± 0.97	6.12 ± 0.84	10.21 ± 0.45	>100

4e	1.80 ± 0.25	6.98 ± 0.21	18.92 ± 0.67	>100
4f	5.18 ± 0.37	13.51 ± 0.33	20.92 ± 0.34	>100
4g	11.51 ± 1.05	15.88 ± 0.65	19.99 ± 0.85	>100
4h	13.65 ± 1.30	18.47 ± 0.53	23.75 ± 0.44	>100
4i	4.21 ± 0.32	13.43 ± 0.21	15.91 ± 0.98	>100
4j	3.25 ± 0.19	10.3 ± 0.34	14.26 ± 0.25	>100
4k	6.38 ± 0.54	8.69 ± 0.88	9.54 ± 1.24	>100
4l	6.80 ± 0.29	9.06 ± 1.54	11.38 ± 2.08	>100
4m	10.22 ± 0.14	15.82 ± 0.58	13.28 ± 0.71	>100
4n	10.47 ± 0.91	14.24 ± 0.82	11.54 ± 1.90	>100
4o	11.61 ± 0.28	12.55 ± 0.35	11.93 ± 1.36	>100
4p	15.11 ± 0.47	17.30 ± 0.51	22.96 ± 0.98	>100
4q	20.84 ± 0.13	15.35 ± 0.32	38.53 ± 0.67	>100
4r	4.43 ± 0.45	11.44 ± 0.69	14.50 ± 2.71	>100
4s	8.29 ± 0.19	22.70 ± 2.09	31.39 ± 2.28	>100
4t	6.87 ± 0.12	10.37 ± 0.21	13.11 ± 0.82	>100
Celecoxib	2.21 ± 1.31	7.51 ± 1.28	0.68 ± 3.14	65.34 ± 0.18

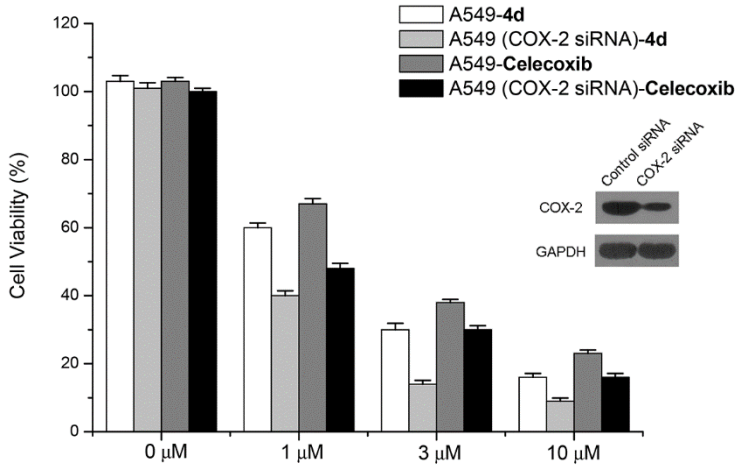

Fig. 2 Knockdown of COX-2 in A549 cells led to remarkable reduction of cell viability after drug treatment.

3.4 Compound 4d reduced the adhesive ability of A549 cells.

Cell adhesion plays a significant role in cancer progression and metastasis, and decreased cell adhesion benefits cancer therapy. In this study, a cell adhesion assay was employed to assess the effects of treatment with compound **4d** and celecoxib at different concentrations for 24 h on the ability of A549 cells to adhere. After harvesting the cells, their adhesive ability to fibronectin and laminin was measured. The results shown in **Fig. 3** indicated that compound **4d** could significantly reduce the adhesive ability of

A549 cells to fibronectin and laminin while the effects of celecoxib were not as striking.

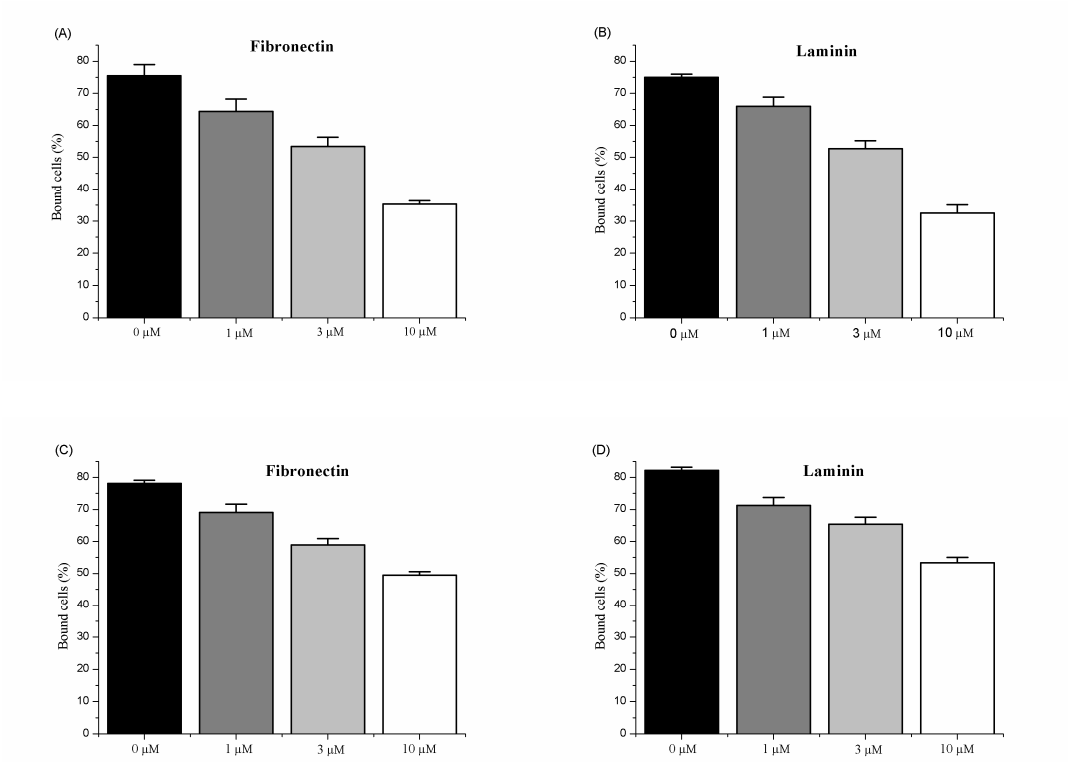

Fig. 3 Influence of compound **4d** and celecoxib on A549 cell adhesion to fibronectin and laminin (A) Influence of compound **4d** on A549 cell adhesion to fibronectin; (B) Influence of compound **4d** on A549 cell adhesion to laminin; (C) Influence of celecoxib on A549 cell adhesion to fibronectin; (D) Influence of celecoxib on A549 cell adhesion to laminin.

3.5 Compound 4d caused cell apoptosis in A549 cells in a dose-dependent manner

To verify whether compound **4d** could inhibit the growth of A549 by inducing apoptosis, flow cytometry was applied, and the results indicated that after treating A549 cells with varying concentrations (0 μM, 1 μM, 3 μM and 10 μM) of **4d** for 24 h, the percentage of apoptotic cells was markedly elevated in a dose-dependent manner. Likewise, A549 cells were treated with corresponding doses of celecoxib (0 μM, 1 μM, 3 μM and 10 μM). As shown in **Fig. 4**, increased concentrations of compound **4d** yielded an increased apoptotic rate of A549 cells. The percentages of cell apoptosis of 8.30%, 19.86%, 34.52% correspond to treatment concentrations of compound **4d** of 1, 3 and 10 μM, respectively. Clearly, compound **4d** can cause cell apoptosis more

effectively than celecoxib. In conclusion, compound **4d** could induce apoptosis in A549 cells in a dose-dependent manner.

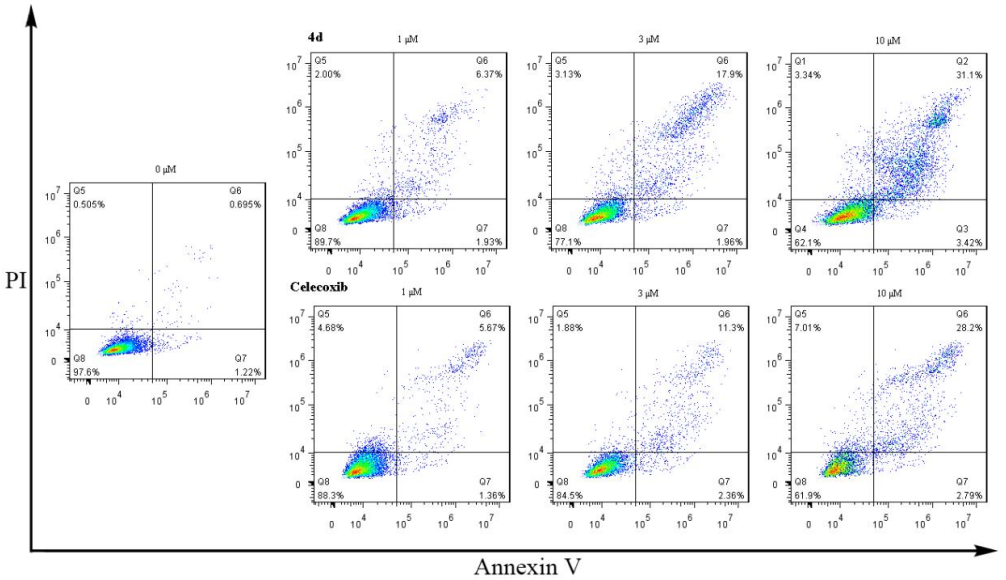

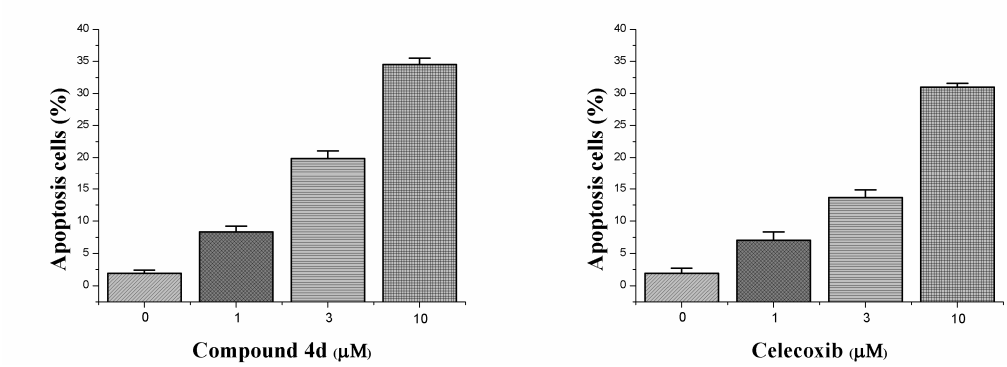

Fig. 4 A549 cells treated with 0, 1, 3 and 10 μM **4d** and celecoxib for 24 h were collected and analysed. The percentage of early apoptotic cells is shown in the lower right quadrant (Annexin V-FITC positive/PI negative cells), and late apoptotic cells are located in the upper right quadrant (Annexin V-FITC positive/PI positive cells). Images are representative of three independent experiments.

3.6 Compound 4d induced cell-cycle arrest in A549 cells in a dose-dependent manner

We further assessed the effect of compound **4d** on the cell cycle to ascertain whether A549 cells are blocked in mitosis. A549 cells were treated with different concentrations (0 μM, 1 μM, 3 μM and 10 μM) of compound **4d** for 24 hours. As illustrated in **Fig. 5**, treatment of A549 cells with compound **4d** led to G2/M arrest in a dose-dependent

manner. Incubation of the cells with 3 μM compound **4d** caused 35.38% of cells to arrest at the G2/M phase. When the concentration of compound **4d** increased to 10 μM, 85.93% of cells were arrested in the G2/M phase. In summary, the accumulation of cells in G2/M phase increased with increased concentration of compound **4d**.

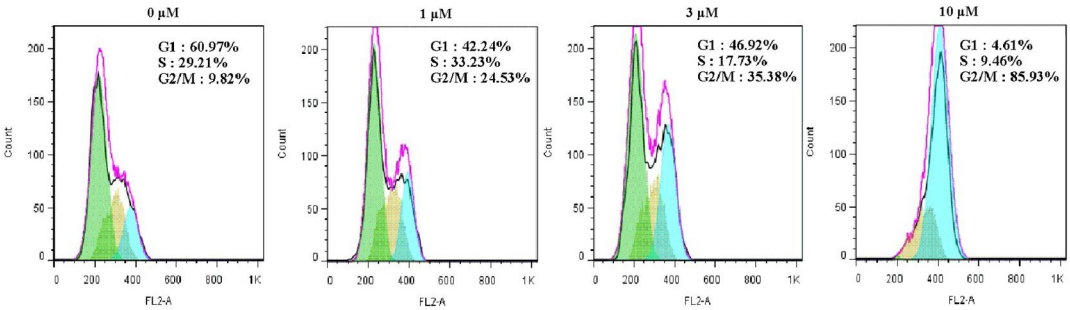

Fig. 5 Effect of compound **4d** on the cell cycle distribution of A549 cells in a dose-dependent manner (0, 1, 3 and 10 μM). Images are representative of three independent experiments. (G1 phase, green; S phase, yellow and G2/M phase, blue).

3.7 *Compound 4d was able to permeate cell membrane and affect cell morphology*

Many studies have applied the strategy of conjugating a fluorescent probe with agents to illustrate the location of these compounds in cells and verify their membrane permeability. Given that our target compounds are generally fluorescent under certain excitations, the conjugation with probe was actually inessential in this assay. Under two-photon excitation, we imaged compound **4d** in A549 cells as shown in **Fig. 6**. No fluorescence was observed in normal A549 cells; however, intense blue fluorescence emerged after incubating A549 cells with 5 μM compound **4d** for 30 min at 37 °C and washed three times with Hepes buffer. The results reflected the ability of **4d** to penetrate cell membrane and its location in cells. Additionally, morphological alterations between A549 cells treated with different concentrations (0 μM, 1 μM, 3 μM and 10 μM) of

compound **4d** for 8 h were observed. DAPI staining was exploited because it can partially penetrate the nucleus to stain nuclear DNA. As shown in **Fig. 7**, while non-treated A549 cells exhibited normal morphology, cells undergoing apoptosis induced by compound **4d** were morphologically varied, with condensed or fragmented nuclei.

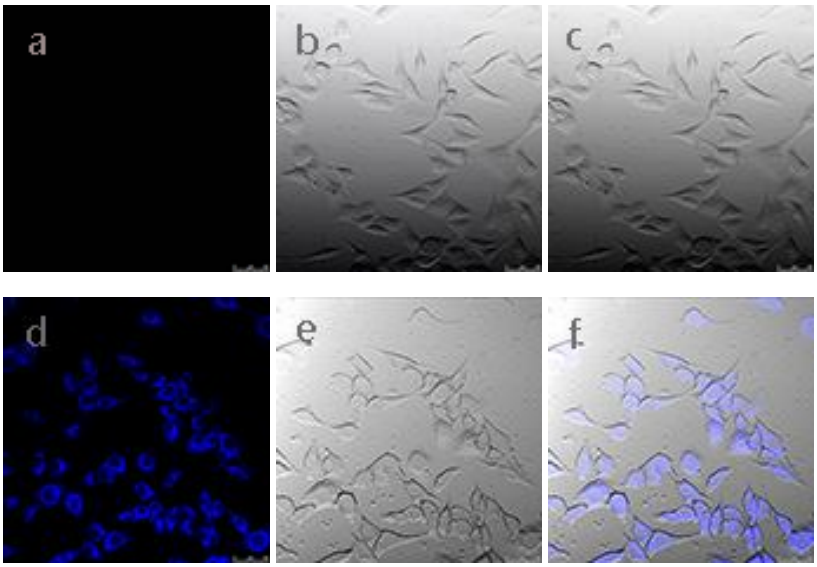

Fig. 6 Confocal microscopy images of A549 live cells visualizing changes in the level of florescence using compound **4d** (5 μM). Images represent emission intensities collected in optical windows between 500 and 600 nm upon excitation at 450 nm for compound **4d**. (a) Two-photon image of A549 cells. λex = 450 nm (emission wavelength from 500 to 600 nm); (b) Bright-field image of A549 cells; (c) Overlay of (a) and (b); (d) Two-photon image of A549 cells incubated with 5 μM compound **4d** after 30 min of incubation, washed with Hepes buffer. λex = 450 nm (emission wavelength from 500 to 600 nm); (e) Bright-field image of A549 cells; (f) Overlay of (d) and (e).

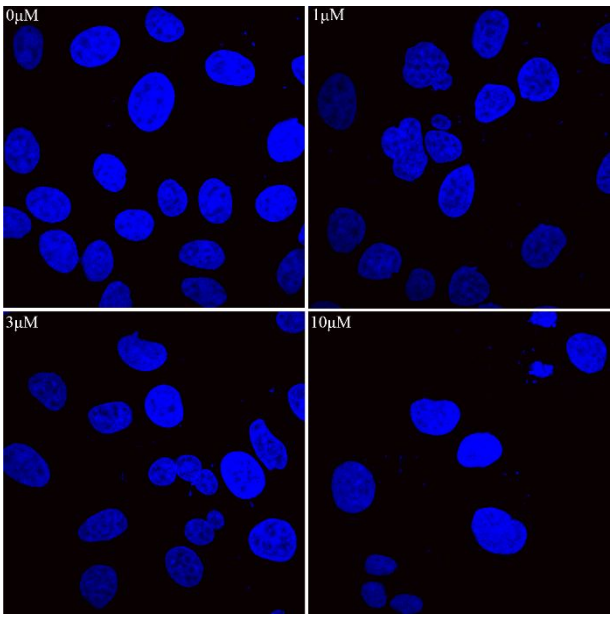

Fig. 7 Morphological changes of DAPI-stained A549 cells after treatment with compound **4d** (0, 1, 3 and 10 μM) observed under confocal microscope.

3.8 Compound 4d reduced the expression of COX-2 in A549 cells.

Western blot analysis was performed to determine whether compound **4d** could suppress the expression of COX-2 in A549 cells. Total proteins were extracted from A549 cells treated with compound **4d** at different concentrations (0 μM, 1 μM, 3 μM and 10 μM). The results were analysed by Image J and indicated that the COX-2 expression of treated cells was inferior to that of untreated cells. As pictured in **Fig. 8**, the expression of COX-2 was reduced as the concentration of compound **4d** increased. In summary, compound **4d** could reduce the protein expression of COX-2 in A549 cells in a dose-dependent manner.

We also performed a Western blot to estimate the transfection efficacy of control siRNA and COX-2 siRNA into A549 cells. The results shown in **Fig. 2** indicated that the interference was performed effectively, and the expression of COX-2 decreased sharply in COX-2 siRNA-mediated cells while it varied undetectably in the control cells.

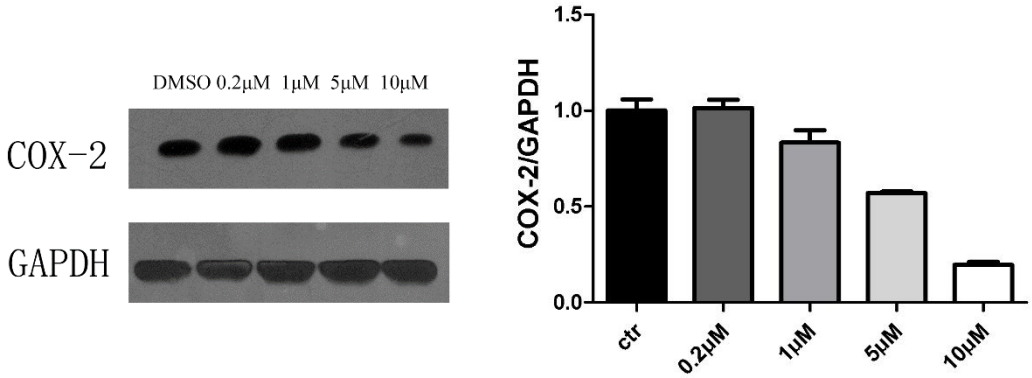

Fig. 8 A549 cells were treated with compound **4d** (0.2, 1, 5 and 10 μM) for 24 h, and the protein level of COX-2 was observed in A549 cells by immunoblotting assay.

3.9 Scaffold modification

Because the scaffold was constructed based on analysis of known COX-2-selective inhibitors, modifications were made to establish a library of small molecules in order to screen for potential anticancer compounds. The members in the library were filtered by Lipinski's “Rule of 5” to ensure good drug characteristics, complementing the docking screening. In addition, the complexity of the synthesis route for these candidates was taken into consideration to ensure synthetic feasibility. A primary screen was conducted to identify the best hits in an *in vitro* COX-2 inhibition assay. Finally, the lead compound with good activity was validated (**Fig. 1**). It possessed better AlogP (with value of 3.736) and binding potential with COX-2 (with binding energy of - 58.44 kcal/mol) than celecoxib (with AlogP of 5.946 and binding energy of - 56.13 kcal/mol). It was then substituted to generate the class of compounds investigated in this study.

3.10 Molecular docking

A docking study was performed iteratively in this study, and the general workflow was described in the method section. In modifying the diarylheterocylic scaffold *in silico*, molecular docking was carried out to fit the scaffold molecules into the activity pocket of COX-2. Afterwards, docking screening was employed to filter the candidates for better binding potential. When the lead compound was finally validated and concomitantly modified to produce the target compounds, docking simulation was also

performed to explore the probable binding modes of these compounds. The latter docking results are summarized in **Table 1**, and a model of compound **4d** docked with COX-2 is depicted in **Fig. 9(A)**. In the binding model, compound **4d** is nicely bound to the active site of the cyclooxygenase-2 by five hydrogen bonds with GLN 178 (angle O · H-N = 125.41°, distance = 2.30 Å), LEU 338 (angle O · H-N = 144.42°, distance = 2.48 Å), SER 339 (angle O · H-N = 146.24°, distance = 2.40 Å), ARG 499 (angle O · H-N = 159.09°, distance = 2.30 Å), and PHE 504 (angle O · H-N = 149.07°, distance = 2.32 Å), and one Pi-Sigma bond with SER 339. Furthermore, other weak interactions, such as van der Waals and carbon-hydrogen bonds, also contributed to the binding affinity of **4d** with COX-2. In **Fig. 9(B)**, 3D models of the interaction between compound **4d** and cyclooxygenase-2 are depicted. The molecular docking suggests that compound **4d** may be a potential COX-2 ligand.

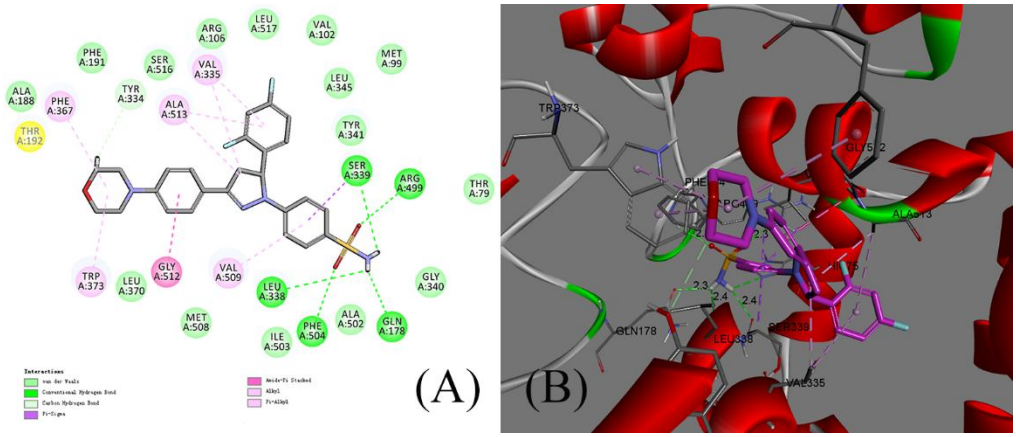

Fig. 9 Binding mode of compound **4d** with COX-2 (PDB code: 3LN1). **(A)** 2D diagram of the interaction between compound **4d** and amino acid residues of the nearby active site. **(B)** 3D diagram of compound **4d** inserted in the COX-2 binding site: for clarity, only interacting residues are displayed.

4. Conclusions

Aberrant expression of COX-2 has been found to be closely related to various types

of cancer, and it is generally accepted that targeting COX-2 is a promising treatment strategy in cancer therapies that has yet to be fully realized. However, the corresponding research is not very elaborate; to further explore the anti-proliferative potential of COX-2 inhibitors, we designed a series of novel dihydropyrazole sulphonamide derivatives with high COX-2 selectivity. These compounds were tested in a series of experiments, and the results indicated that some compounds may be promising in drug development. Compound **4d** is the most impressive, with a notable biological profile. Analysis revealed that it has a lower AlogP value compared with the famous COX-2 agent celecoxib, along with a higher binding affinity to COX-2. The advantages of **4d** were also highlighted by bioassays. Against COX-2 and the A549 cancer cell line, **4d** demonstrated better inhibitory potency than celecoxib. Assisted by siRNA-mediated COX-2 knockdown, **4d** was shown to exert its anticancer effect through COX-2 inhibition. The initial investigation also suggested satisfying selectivity and safety. While no overt adhesive reduction was observed in the celecoxib-treated group, **4d** was found able to decrease the adhesive ability of A549 cells. Compound **4d** could induce apoptosis of A549 cell and cell cycle arrest in G2/M phase in a dose-dependent manner. The morphological alterations of A549 cells affected by compound **4d** can be directly perceived by confocal microscopy observation. The western blot results also demonstrated that compound **4d** could reduce the expression of COX-2 in A549 cells, hinting that a more complicated mechanism is involved in its inhibitory activities. In summary, we reported a series of dihydropyrazole sulphonamide derivatives, along with their design and bioactivities. We hope that this study will benefit the study of

cancer treatment through COX-2 inhibition.

Conflict of interest

The authors have no relevant affiliations or financial involvement with any organization or entity with a financial interest in or financial conflict with the subject matter or materials discussed in the manuscript.

Acknowledgment

The work was financed by a grant (No. J1103512) from National Natural Science Foundation of China.

References

1. Y. Shamsudin Khan, H. Gutiérrez-de-Terán, L. Boukharta, and J. Åqvist. Toward an optimal docking and free energy calculation scheme in ligand design with application to COX-1 inhibitors. Journal of chemical information and modeling. 54:1488-1499 (2014).
2. Q. Peng, S. Yang, X. Lao, W. Tang, Z. Chen, H. Lai, J. Wang, J. Sui, X. Qin, and S. Li. Meta-analysis of the association between COX-2 polymorphisms and risk of colorectal cancer based on case–control studies. PloS one. 9:e94790 (2014).
3. R.H. Tolba, N. Fet, K. Yonezawa, K. Taura, A. Nakajima, K. Hata, Y. Okamura, H. Uchinami, U. Klinge, and T. Minor. Role of preferential cyclooxygenase-2 inhibition by meloxicam in ischemia/reperfusion injury of the rat liver. European Surgical Research. 53:11-24 (2014).
4. E. Yıldırım, O. Sağıroğlu, F.S. Kılıç, and K. Erol. Effects of nabumetone and dipyrone on experimentally induced gastric ulcers in rats. Inflammation. 36:476-481 (2013).
5. A. Greenhough, H.J. Smartt, A.E. Moore, H.R. Roberts, A.C. Williams, C. Paraskeva, and A. Kaidi. The COX-2/PGE2 pathway: key roles in the hallmarks of cancer and adaptation to the tumour microenvironment. Carcinogenesis. 30:377-386 (2009).
6. N. Ghosh, R. Chaki, V. Mandal, and S.C. Mandal. COX-2 as a target for cancer chemotherapy. Pharmacological reports. 62:233-244 (2010).
7. L. Minghetti. Cyclooxygenase‐2 (COX‐2) in inflammatory and degenerative brain diseases. Journal of Neuropathology & Experimental Neurology. 63:901-910 (2004).
8. L.M. Jacksonand C.J. Hawkey. COX-2 selective nonsteroidal anti-inflammatory drugs. Drugs. 59:1207-1216 (2000).
9. J.J. Talley, D.L. Brown, J.S. Carter, M.J. Graneto, C.M. Koboldt, J.L. Masferrer, W.E. Perkins, R.S. Rogers, A.F. Shaffer, and Y.Y. Zhang. 4-[5-Methyl-3-phenylisoxazol-4-yl]-benzenesulfonamide, valdecoxib: a potent and selective inhibitor of COX-2. Journal of medicinal chemistry. 43:775-777 (2000).
10. C.A. Birbara, A.D. Puopolo, D.R. Munoz, E.A. Sheldon, A. Mangione, N.R. Bohidar, G.P. Geba, and E.P.S. Group. Treatment of chronic low back pain with etoricoxib, a new cyclo-oxygenase-2 selective inhibitor: improvement in pain and disability—a randomized, placebo-

controlled, 3-month trial. The journal of pain. 4:307-315 (2003).

11. S.-J. Cho, N. Kim, J.S. Kim, H.C. Jung, and I.S. Song. The anti-cancer effect of COX-2 inhibitors on gastric cancer cells. Digestive diseases and sciences. 52:1713-1721 (2007).

12. L. Tao, S. Wang, Y. Zhao, X. Sheng, A. Wang, S. Zheng, and Y. Lu. Phenolcarboxylic acids from medicinal herbs exert anticancer effects through disruption of COX-2 activity. Phytomedicine. 21:1473-1482 (2014).

13. A. Kirane, J.E. Toombs, K. Ostapoff, J.G. Carbon, S. Zaknoen, J. Braunfeld, R.E. Schwarz, F.J. Burrows, and R.A. Brekken. Apricoxib, a novel inhibitor of COX-2, markedly improves standard therapy response in molecularly defined models of pancreatic cancer. Clinical Cancer Research. 18:5031-5042 (2012).

14. M. Vosooghiand M. Amini. The discovery and development of cyclooxygenase-2 inhibitors as potential anticancer therapies. Expert opinion on drug discovery. 9:255-267 (2014).

15. K. Ng, J.A. Meyerhardt, A.T. Chan, K. Sato, J.A. Chan, D. Niedzwiecki, L.B. Saltz, R.J. Mayer, A.B. Benson, and P.L. Schaefer. Aspirin and COX-2 Inhibitor Use in Patients With Stage III Colon Cancer. Journal of the National Cancer Institute. 107:dju345 (2015).

16. A. Okamoto, T. Shirakawa, T. Bito, K. Shigemura, K. Hamada, A. Gotoh, M. Fujisawa, and M. Kawabata. Etodolac, a selective cyclooxygenase-2 inhibitor, induces upregulation of E-cadherin and has antitumor effect on human bladder cancer cells in vitro and in vivo. Urology. 71:156-160 (2008).

17. A. Zarghiand S. Arfaei. Selective COX-2 inhibitors: a review of their structure-activity relationships. Iranian journal of pharmaceutical research: IJPR. 10:655 (2011).

18. F. Wuest, T. Kniess, R. Bergmann, and J. Pietzsch. Synthesis and evaluation in vitro and in vivo of a 11 C-labeled cyclooxygenase-2 (COX-2) inhibitor. Bioorganic & medicinal chemistry. 16:7662-7670 (2008).

19. K.A. Abouzid, N.A. Khalil, E.M. Ahmed, H.A.A. El-Latif, and M.E. El-Araby. Structure-based molecular design, synthesis, and in vivo anti-inflammatory activity of pyridazinone derivatives as nonclassic COX-2 inhibitors. Medicinal chemistry research. 19:629-642 (2010).

20. A. Pacelli, J. Greenman, C. Cawthorne, and G. Smith. Imaging COX‐2 expression in cancer using PET/SPECT radioligands: current status and future directions. Journal of Labelled Compounds and Radiopharmaceuticals. 57:317-322 (2014).

21. S. Ovais, S. Yaseen, R. Bashir, P. Rathore, M. Samim, S. Singh, V. Nair, and K. Javed. Synthesis and anti-inflammatory activity of celecoxib like compounds. Journal of enzyme inhibition and medicinal chemistry. 28:1105-1112 (2013).

22. S. Pericherla, J. Mareddy, D. Rani, P.V. Gollapudi, and S. Pal. Chemical modifications of nimesulide. Journal of the Brazilian Chemical Society. 18:384-390 (2007).

23. N. Handler, W. Jaeger, H. Puschacher, K. Leisser, and T. Erker. Synthesis of novel curcumin analogues and their evaluation as selective cyclooxygenase-1 (COX-1) inhibitors. Chemical and pharmaceutical bulletin. 55:64-71 (2007).

24. P.A. Connolly, M.M. Durkin, A.M. LeMonte, E.J. Hackett, and L.J. Wheat. Detection of histoplasma antigen by a quantitative enzyme immunoassay. Clinical and Vaccine Immunology. 14:1587-1591 (2007).

25. M. Oka, S. Maeda, N. Koga, K. Kato, and T. Saito. A modified colorimetric MTT assay adapted for primary cultured hepatocytes: application to proliferation and cytotoxicity assays. Bioscience, biotechnology, and biochemistry. 56:1472-1473 (1992).